

Corrosion Resistance of Novel Coatings on Ferritic Steels for Oxycombustion–Supercritical Steam Boilers: Preliminary Results

Alina Agüero¹ · Ignacio Baraibar¹ · Vanessa González¹ · Raúl Muelas² · Daniel Plana¹

Received: 23 June 2015 / Published online: 23 July 2015
© Springer Science+Business Media New York 2015

Abstract Increasing the efficiency of coal fired steam power plants is an important contribution towards clean coal power. In fact, new ferritic steels are expected to withstand 325 bar and 650 °C. Moreover, in order to facilitate CO₂ capture oxygen can be used instead of air for combustion (oxycombustion) so that no NO_x emissions are produced. Boiler components, such as superheater tubes, are exposed to both steam and fireside corrosion and at higher temperatures, ferritic steels corrode at very fast rates under both atmospheres. A solution can be found in the use of protective coatings, a number of which, applied by techniques capable of depositing said coatings both on the inner and outer surfaces of tubes, are being studied within nationally and European funded projects. In particular, two new Ni and Cr modified aluminide coatings deposited on P92 by non-line-of-sight hybrid processes have been produced and the preliminary results of on-going laboratory testing, both under oxycombustion model atmospheres as well as under pure steam at 650 °C are promising, in particular those exhibited by the Cr enriched aluminide coating. Moreover, results obtained in a pilot oxycombustion boiler operated by CIUDEN in Leon, Spain are also shown.

Keywords Coatings · Aluminides · Boilers · Steam oxidation · Oxycombustion · Fireside corrosion

✉ Alina Agüero
agueroba@inta.es

¹ Instituto Nacional de Técnica Aeroespacial, Ctra. Ajalvir Km 4, 28850 Torrejón de Ardoz, Spain

² Ingeniería de Sistemas para la Defensa de España SA, Calle Beatriz de Bobadilla No. 3, 28040 Madrid, Spain

Introduction

The need to produce energy more efficiently and with reduced environmental impact, has become evident. Producing energy efficiently by means of burning any fuel leads to increasingly extreme conditions, imposing more demanding performances on materials, such as higher temperatures and pressures, and more corrosive atmospheres. State-of-the-art steels allow steam parameters up to 300 bar and 600–620 °C [1, 2] and the new currently ongoing developments will lead to further reductions not only of emissions but also of costs. The new ferritic steels are expected to withstand 325 bar and 650 °C allowing to increase efficiency of steam power plants from 46 % to approximately 50 %, and reducing CO₂ emissions to 8 %. An alternative to facilitate CO₂ capture is the use of oxygen instead of air for combustion (oxycombustion) of any fuel in the boiler of steam power plants. As the nitrogen presence on the combustion atmosphere is almost zero, the NO_x emissions are drastically reduced and it is then possible to separate and capture practically 100 % of the produced CO₂ [3]. However, oxycombustion atmospheres are richer in CO₂, SO₂ and water vapor and under this atmosphere corrosion rates are expected to be higher [4, 5]. Moreover the ash composition is also different [6–8]. In addition when supercritical steam conditions are required, and the components are exposed to temperatures higher than 600 °C steam oxidation is also expected to increase. In fact, some boiler components, such as the superheater tubes, are exposed to both steam and fireside corrosion at these high temperatures, and ferritic steels corrode at very fast rates under both atmospheres. In addition, results indicate that any attempts to design ferritic steels to simultaneously increase the creep strength and decrease the oxidation rates have failed so far. A solution may be to use materials with lower thermal conductivity and higher cost (austenitic steels and Ni base alloys). However, recent results have indicated that high Cr steel such as VM12 and even austenitic 316 NL develop thick oxide scales after relatively short exposure times when exposed to supercritical steam at high pressures [9].

Alternatively, high creep strength ferritic alloys can be designed relying on the use of coatings for oxidation protection, such as in the hot section of gas turbines, where coatings have been employed for over 50 years, to protect high strength superalloys components from high temperature corrosion.

Laboratory as well as field testing, have demonstrated that coatings can significantly reduce steam oxidation at 600–650 °C [10, 11] but the behavior of coatings under oxycombustion atmosphere is less known. In the case of heat exchangers, the same coating could be ideally applied both on the external and internal surfaces. By applying Al containing slurries to form Fe aluminide coatings after a suitable heat treatment, this can be achieved. These coatings are already known to be very stable both under steam and conventional fire-side corrosion atmospheres at 650 °C [12, 13]. However degradation occurs by Al interdiffusion which may have two negative effects: (1) it causes Al depletion at the surface, resulting in an Al content lower than the critical value required to maintain a stable protective alumina layer and (2) it causes the precipitation of AlN, depleting the steel from N and possibly affecting the mechanical properties of the material after

long term. Moreover, these coatings exhibit through-thickness cracks due to thermal expansion coefficient mismatch between the iron aluminide phases, in particular brittle Fe_2Al_5 , and the substrate (Fig. 1). It has already been shown that for an Al content between 4 and 7 wt.% instead of alumina, less protective, faster growing Fe, Al mixed oxides begin to form in a coating with an initial 4 wt.% Cr content [14].

A number of new coatings, applied by techniques capable of depositing said coatings both on the inner and outer surfaces of heat exchanger tubes, are being studied within nationally and European funded projects [15, 16]. In particular, two new Ni and Cr modified aluminide coatings deposited on P92 by non-line-of-sight hybrid processes have been produced in order to reduce diffusion and to avoid the presence of cracks. The microstructures of the new coatings are shown as well as the preliminary results of on-going laboratory testing both under oxycombustion model atmospheres as well as under pure steam at 650 °C. The already mentioned slurry aluminide coating as well as uncoated P92 were also tested for comparison purposes. Finally, results obtained in a pilot oxycombustion boiler operated by CIUDEN in Leon, Spain will also be shown. Results indicate that some of the tested coatings exhibit very stable behavior under both atmospheres at 650 °C.

Experimental Procedures

Substrate

Samples coupons ($20 \times 10 \times 3$ mm) were machined from tubular sections of P92 (C: 0.1, Mn: 0.5, Si: 0.03, Cr: 8.8, Ni: 0.06, Mo: 0.4, W: 1.8, V: 0.20, S: 0.006, N:

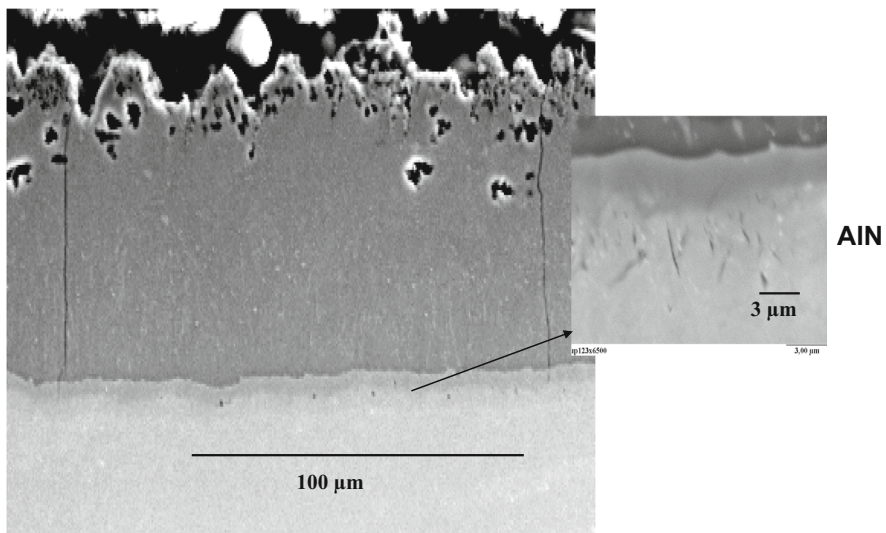


Fig. 1 Slurry aluminide coating on P92

0.046 Fe: bal., wt.%,) obtained from Vallourec Mannesmann. Prior to coating, all samples for all coatings were ground (Struers 180) and solvent degreased.

Coatings

Two new Cr and Ni modified diffusion aluminide coatings have been deposited employing combinations of non-line-of-sight different processes, in order to reduce diffusion and to avoid cracks exhibited by the slurry deposited aluminide coating. The already studied slurry aluminide was also included as a reference for comparison purposes.

Slurry Aluminide

The Al slurry is a Cr(VI) free water base proprietary composition containing only inorganic compounds. The Al slurry was applied by spraying and the coated samples were subjected to a diffusion heat treatment performed under argon flow at 700 °C for 10 h.

Cr Enriched Aluminide

This coating was also applied in two steps: (1) Cr was initially deposited by a chromium based proprietary slurry followed by a diffusion heat treatment at 1050 °C for 5 h and (2) the sample was later aluminized by means of applying an Al slurry followed by a diffusion heat treatment at 1050 °C for 35 min.

Ni Aluminide

This coating was applied in two steps: (1) Ni was initially deposited by electroless deposition from a NiSO₄, (NH₄)₃C₆H₅O₇ and NaH₂PO₂·H₂O solution at 50 °C followed by a heat treatment at 700 °C for 10 h and (2) the sample was subsequently aluminized by means of applying an Al slurry followed by a diffusion heat treatment at 700 °C for 10 h.

Testing

Steam Oxidation (In the Laboratory)

Uncoated substrates were ground (Struers 120) prior to testing. The schematics of the closed loop laboratory rig employed at INTA are shown elsewhere [9]. Prior to testing, laboratory air is displaced from the specimen chamber by means of N₂ which is kept flowing while heating up to the test temperature (approximately at a rate of 600 °C/h). Once the test temperature has been reached, the N₂ flow is stopped and pure steam is introduced at a linear velocity of 7 cm/s. To carry out weight measurements or to remove samples, the furnace is cooled to about 300 °C under steam and, before the specimens are removed, the steam flow is replaced by N₂. The

reheat cycle is also carried out under N_2 atmosphere up to $650\text{ }^\circ\text{C}$ at which point steam is introduced.

Fire-Side Corrosion (In the Laboratory)

The test was performed using an experimental especially designed rig with four independent lines for H_2O , SO_2 , O_2 , N_2 and CO_2 feeding a tubular reactor placed in a furnace (Fig. 2). The gas composition is shown in Table 1. The samples were placed in alumina crucibles and exposed to the flowing gaseous atmosphere at atmospheric pressure and $650\text{ }^\circ\text{C}$. The exhaust gas was neutralized by bubbling it through alkaline solutions. The test begins by flowing nitrogen for 1 h while the furnace is heating up to the test temperature. Once the test temperature is reached, the nitrogen is closed and the corrosive gases and water vapor are introduced at a linear velocity of 3 cm/s. Every 7 days the test is stopped to weight the specimens by cutting the corrosive gas mixture and turning the furnace off and introducing N_2 . After approximately 2 h once the temperature is $300\text{ }^\circ\text{C}$ or lower the samples are removed.

Pilot Plant Testing

The test was carried out in a pilot fluidized bed combustion boiler burning coal and operating in oxycombustion conditions in CIUDEN's pilot plant (Leon, Spain). Reheat tubes were coated and tested at plant conditions. The tubes were exposed to 10 days at $650\text{ }^\circ\text{C}$ under a pure coal burning atmosphere plus another 10 days at the same temperature but employing a mixture of coal and biomass as fuel.

Characterization

The oxidized specimens were characterized by light optical microscopy (Leica MEF 4) and field emission scanning electron microscopy (FESEM) employing a JEOL

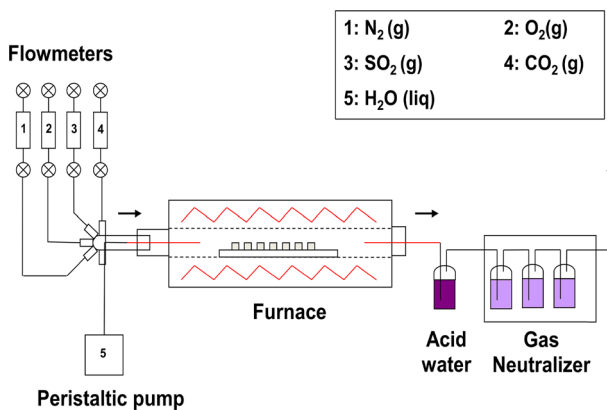


Fig. 2 Schematics of the laboratory oxycombustion test rig

Table 1 Composition of the oxyfuel model atmosphere for the fire-side corrosion test

	CO ₂	H ₂ O	N ₂	O ₂	SO ₂
Vol.%	60	30	7	2	1

JSM 840 system equipped with an energy dispersive X-ray spectrometer (EDS) KEVEX MICROANALYST 8000 with a RÖNTEC signal processor.

Results

Morphology and Microstructure of the Coatings

Cr Enriched Aluminide Coating

In order to avoid crack formation, a higher temperature heat treatment leading to lower Al containing phases such as FeAl instead of the brittle Fe₂Al₅ was used. Moreover, the coating was enriched in Cr as the surface Al content was expected to be lower than that of the original aluminide coating showed in Fig. 1. It is known that the critical amount of Al required to maintain a protective alumina scale is related to the Cr content, the higher the Cr the lower the critical Al content [17]. The Cr enriched aluminide was deposited in a series of steps. Initially, a Cr slurry was applied to P92, followed by heat treating at 1050 °C (Fig. 3). In this manner, the alloy Cr content ($\cong 9$ wt.%) was increased to 15–18 wt.% at the surface. The material affected by Cr enrichment consisted of very large grains reaching approximately a depth of ~ 60 μm . Cr enrichment within the grain boundaries could

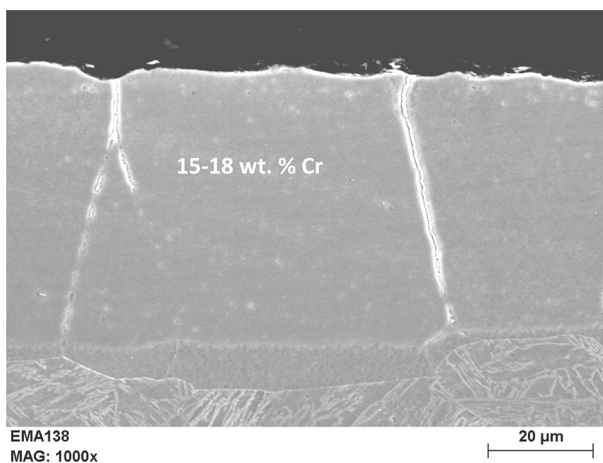


Fig. 3 Cr enriched P92 deposited by slurry and heat treated at 1050 °C

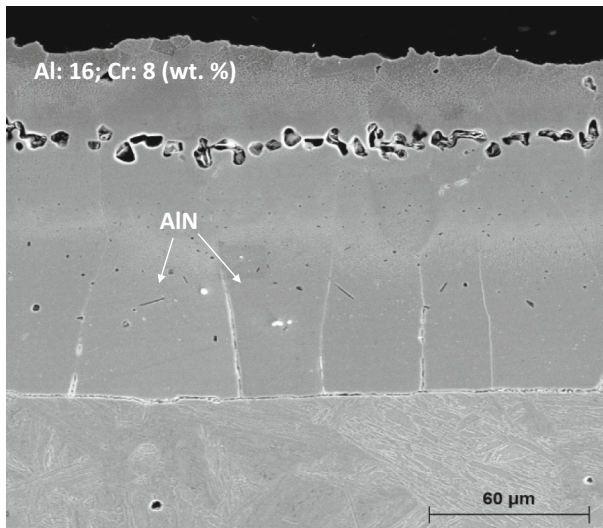


Fig. 4 Cr enriched aluminide coating deposited by slurry aluminizing at 1000 °C on previously chromized P92

be observed perhaps due the precipitation of Cr carbides. The Cr content is constant along the depth of the chromized zone. In the second step, aluminization was carried out also by means of slurry application followed by a heat treatment in this case at 1050 °C (Fig. 4). The new coating exhibits and outer 50–60 μm layer with 16 wt.% of Al and 10 wt.% of Cr and a thicker, large grain zone with a decreasing Al gradient, reaching 2 wt.%, at about 300 μm from the surface, at the interface with the substrate. AlN acicular precipitates are also observed in this zone and Cr enrichment within the grain boundaries could also be measured. The top layer is composed of β FeAl as shown by XRD and lower intensity peaks corresponding to Fe₃Al can also be observed (Fig. 5). Between the two zones significant Kirkendall porosity can be observed, likely as a result of faster Fe outwards diffusion as compared with Al diffusion.

Ni Aluminide

This coating was also obtained in several steps: (1) application of 25 μm of Ni(P) by means of electroless deposition from a P containing precursor, (2) a diffusion heat treatment at 700 °C, (3) application of an Al slurry and (4) a final heat treatment at 700 °C. After step 2, interdiffusion between Ni and Fe takes place as shown in Fig. 6. The diffused coating thickness does not vary significantly from the original 25 μm but four different zones with different grain sizes can be observed: (1) a top P rich layer into which some Fe has diffused, covered by a thin oxide rich in Ni, Fe and Cr, (2) an intermediate small grain zone richer in Fe and also with about 2 wt.% in Cr, (3) a larger grain zone with more Fe and Cr but still very rich in Ni and (4) an inner very finely grain zone with less Ni. After aluminizing, and the final heat

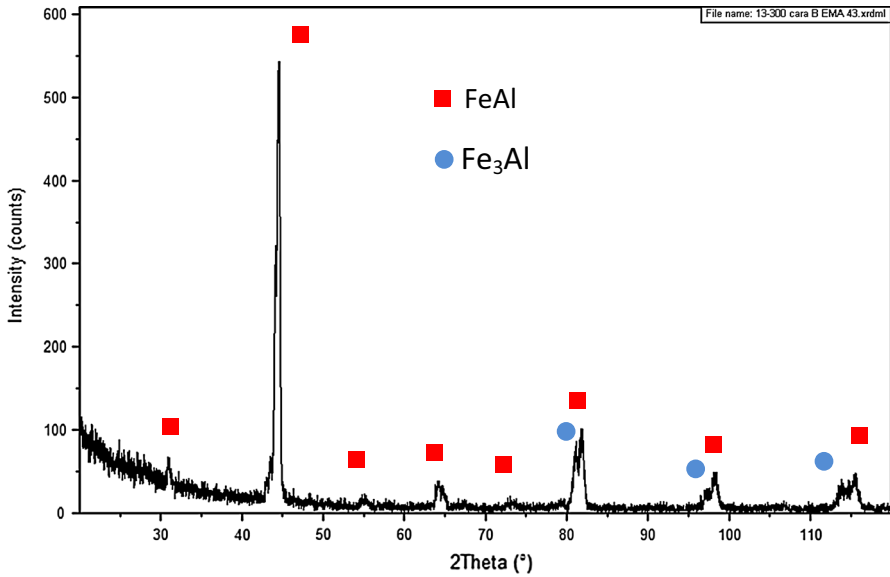


Fig. 5 XRD pattern of the Cr enriched aluminide coating

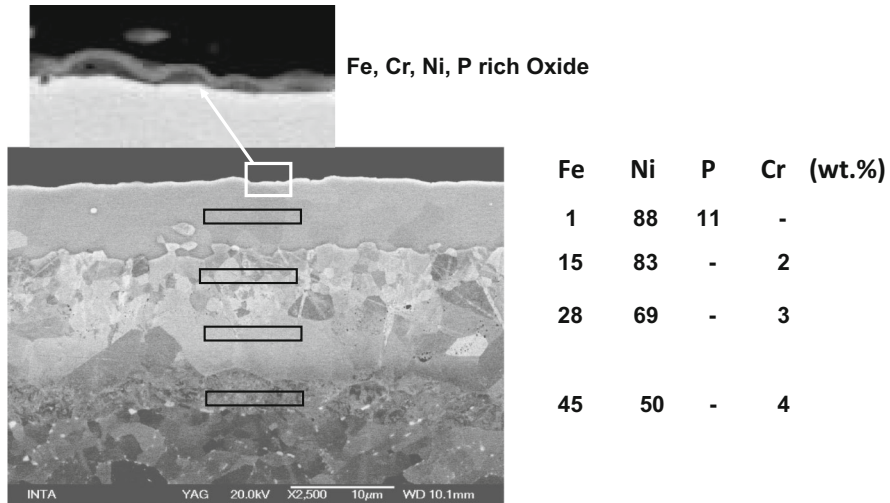


Fig. 6 P92 coated with Ni(P) by electroless deposition followed by a diffusion heat treatment at 700 °C under argon flow. The analysis data correspond to the shown zones within the coatings

treatment at 700 °C, a coating comprising distinct zones was obtained as shown in Fig. 7. According to the XRD pattern shown in Fig. 8, as well as EDS analysis, the outer and middle layers are composed of Ni₂Al₃ and AlP (there is <1 wt.% in P is detected within the outer layer and 4 in the middle one), whereas the internal zone may corresponds to (Ni,Fe)₂Al₃ also containing P. The middle and internal zones

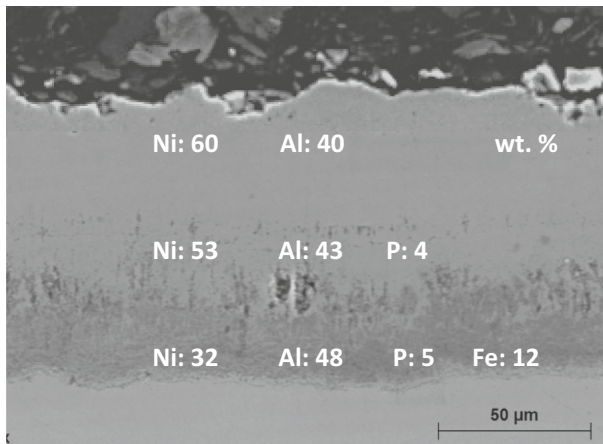


Fig. 7 Ni aluminide coating deposited by slurry aluminizing the electroless Ni(P) diffused coating deposited on P92

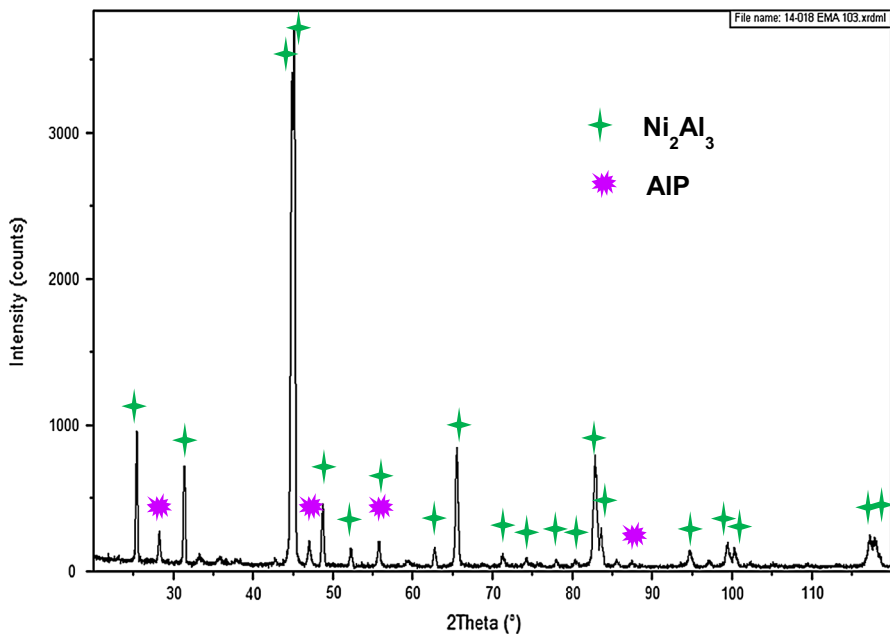


Fig. 8 XRD pattern of the Ni aluminide coating

exhibit porosity, and within the internal zone very small dark precipitates can also be observed, but could not be analysed due to the very small size. Ni aluminides are less brittle than Fe aluminides and accordingly, no cracks are observed in this coating.

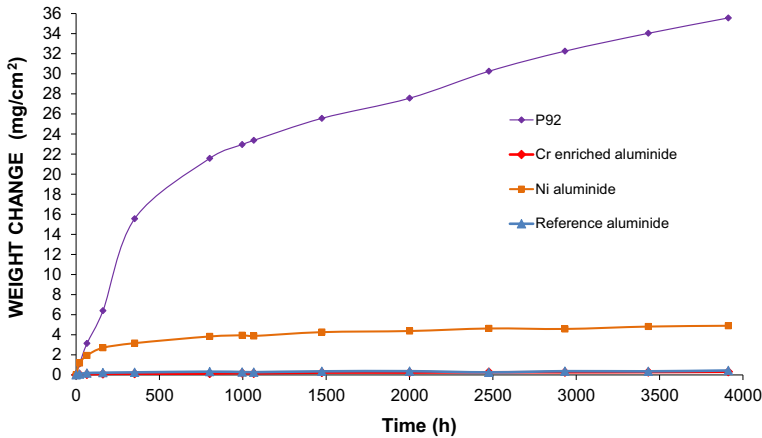


Fig. 9 Mass variation of coated and uncoated P92 exposed to pure flowing steam at 650 °C

Oxidation Behaviour of the Coatings in Steam

This test was performed under 100 % atmospheric, pure flowing steam. The preliminary results indicate that all coatings are protective in comparison with uncoated P92 after at least 4000 h as shown in Fig. 9.

As expected, uncoated P92 develops thick oxides even after relatively short exposure times as shown in Fig. 10a and b, where samples exposed to 1000 and 2000 h are exhibited. A typical dual layered oxide forms with an external Fe_3O_4 layer and an inner mixture of $(\text{Fe}, \text{Cr})_3\text{O}_4$ and Fe_3O_4 growing both inwards and outwards respectively, as function of exposure time [18]. Cracks and pores can be observed in particular within the outer growing Fe_3O_4 layer.

The reference, pure aluminide coating exhibits significant microstructural changes as already mentioned, even after only 1000 h, due to Al and Fe inter-diffusion as seen in Fig. 11a. The inner FeAl zone has grown in thickness at the expense of Fe_2Al_5 and islands of FeAl can also be observed within the remaining Fe_2Al_5 layer. Although through-thickness cracks develop in this coating during the diffusion heat treatment, there are no signs of further propagation into the substrate or of substrate corrosion. After 2000 h (Fig. 11b) further growth of FeAl is observed and in both samples, pores seem to have formed both within the coating as well as in the coating-substrate interface. In addition, the AlN precipitation zone under the coating has increased from initially ~ 5 to 25 μm after 1000 h and to 40 μm after 2000 h. This zone indicates the depth reached by Al as it diffuses inwards.

In contrast, the Cr enriched aluminide coating exhibits no microstructural or compositional changes, as it can be observed in the cross-sections of the samples taken after 1000 and 2000 h (Fig. 12), which are exactly the same as that of the initial coating. The weight variation is low and similar to that of the reference aluminide indicating an excellent behavior from the microstructure and the chemical stability perspectives.

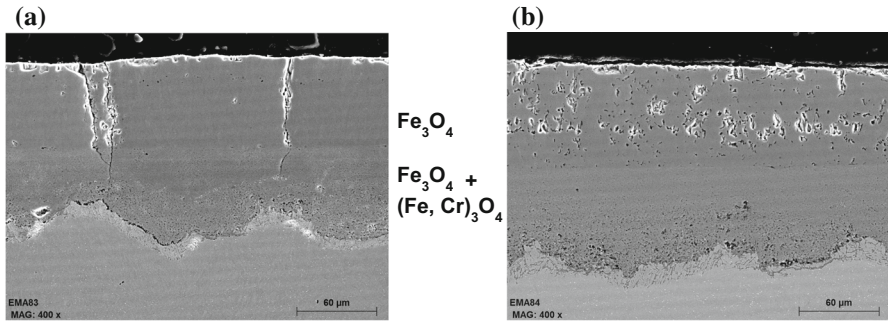


Fig. 10 P92 exposed to steam at 650 °C. **a** For 1000 h and **b** for 2000 h

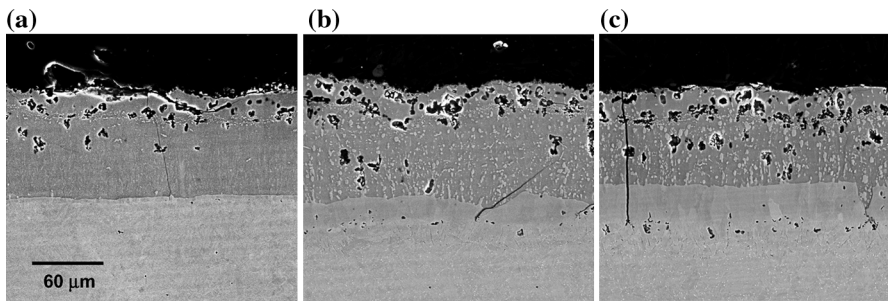


Fig. 11 Fe aluminide coating. **a** As deposited, **b** and **c** after 1000 and 2000 h of exposure to steam at 650 °C respectively

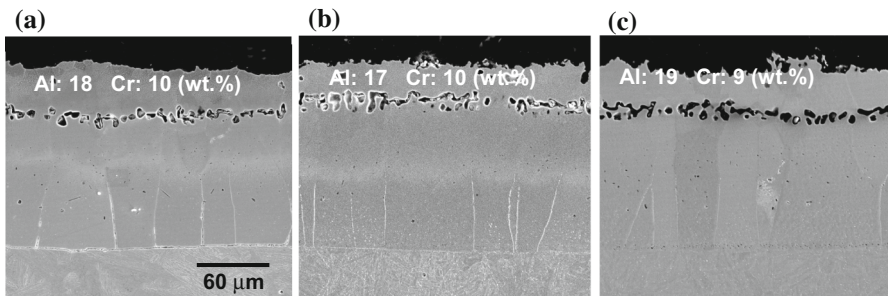


Fig. 12 Cr enriched aluminide coating. **a** As deposited, **b** and **c** after 1000 and 2000 h of exposure to steam at 650 °C, respectively

On the other hand, the Ni Aluminide coating exhibited initially higher weight gain but tending to stabilize after the first 1000 h. Surprisingly, the image of this coating after 1000 h of exposure to steam, showed a quite high degree of oxidation in the internal layers of the coating, reaching all the way into the substrate (Fig. 13b). Puzzling, the outer Ni aluminide as well as some of the middle Fe, Ni

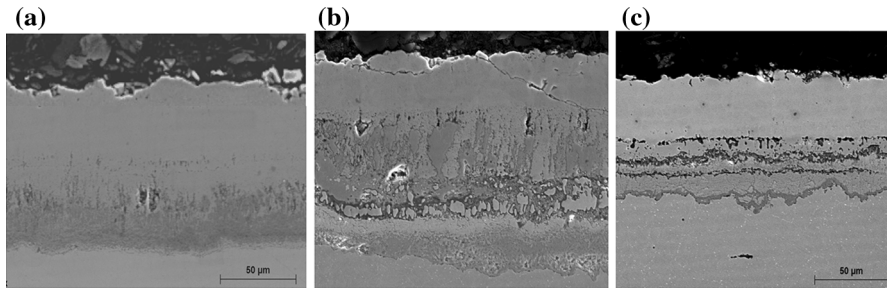


Fig. 13 Ni aluminide coating. **a** As deposited, **b** and **c** after 1000 and 2000 h of exposure to steam at 650 °C, respectively

aluminide remain un-oxidized as shown by the element mapping presented in Fig. 14. Moreover, the sample exposed for 2000 h experienced less oxidation than that exposed to 1000 h. This may be indicative that steam could reach the inner zone of the coatings by imperfections such as pores present in the top layer. Element mapping (Fig. 15) and EDS analysis of this sample shows a Ni aluminide external layer with Fe increasing from the surface (almost none) to about 15 wt.% at the interface with the next layer. Then there is a thin oxide mostly containing Fe and P and Al on top of a layer rich in Fe (80 wt.%) and P (15 wt.%) with some Ni (5 wt.%). Finally, under this zone, there is a multilayered oxide with high amounts of Cr and Fe and some Ni and P. It appears that in contrast with the sample exposed for lower time (1000 h), only the coating middle section has oxidized and a Cr rich thin oxide can also be observed at the corresponding oxide-substrate interface under which Cr depletion is evident. This oxide once it forms, may be protective as after the initial oxidation period, the oxidation rate is significantly reduced.

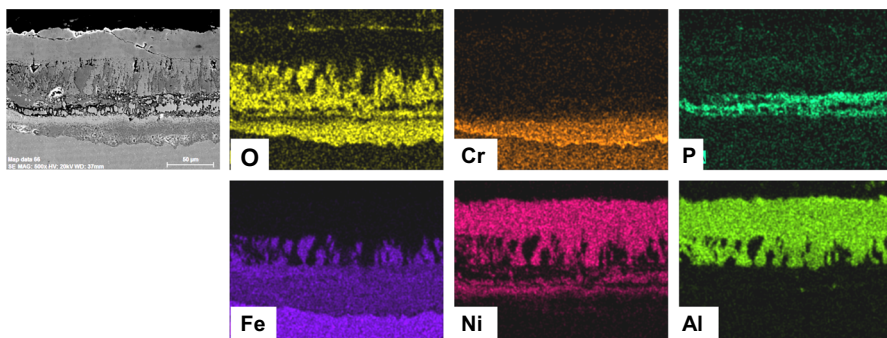


Fig. 14 EDS element mapping of the cross section of the Ni aluminide coating exposed to steam at 650 °C for 1000 h

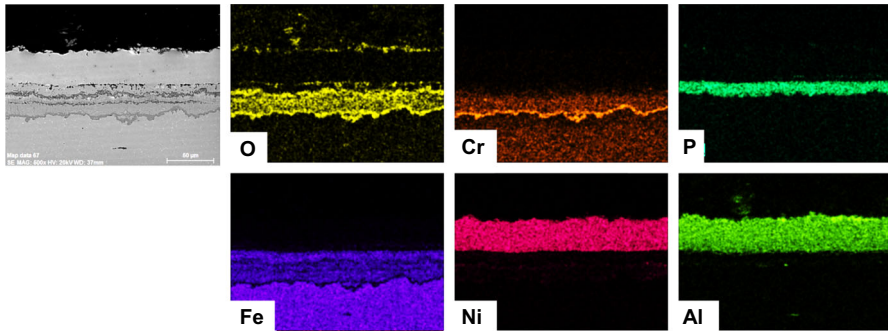


Fig. 15 EDS element mapping of the cross section of the Ni aluminide coating exposed to steam at 650 °C for 2000 h

Oxidation Behaviour of the Coatings in Fire-Side Oxycombustion

Samples of uncoated P92, the reference aluminide coating and the Cr enriched aluminide are being exposed at 650 °C, to a model oxycombustion atmosphere shown in Table 1. The Ni aluminide coating was not tested due to the disappointing results obtained on exposure to steam. The mass variation as a function of time is shown in Fig. 16.

P92 exhibits a high degree of corrosion evidenced by the high mass increase and the thickness of the oxide forms after only 168 h. Hematite (Fe_2O_3) can be observed at the surface, on top of magnetite (Fe_3O_4) and a mixed spinel zone (Fig. 17). The presence of sulfur at the surface as well as in the form of precipitates mainly localized at the oxide-substrate interface could be observed, as shown in the element

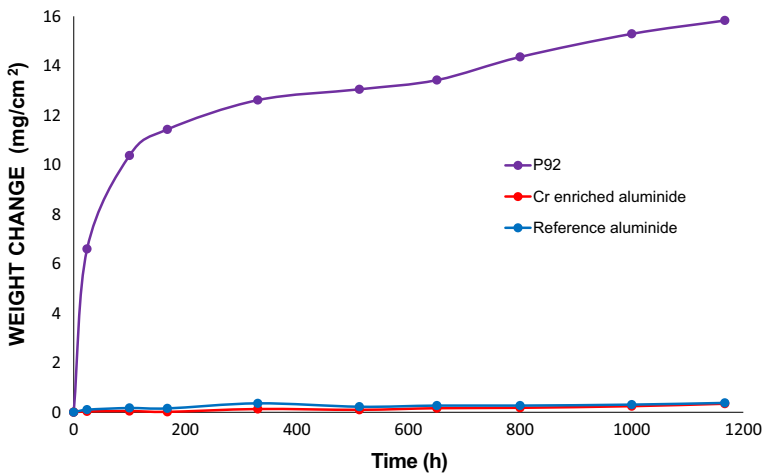


Fig. 16 Mass variation of coated and uncoated P92 exposed to a model oxycombustion atmosphere (Table 1) at 650 °C

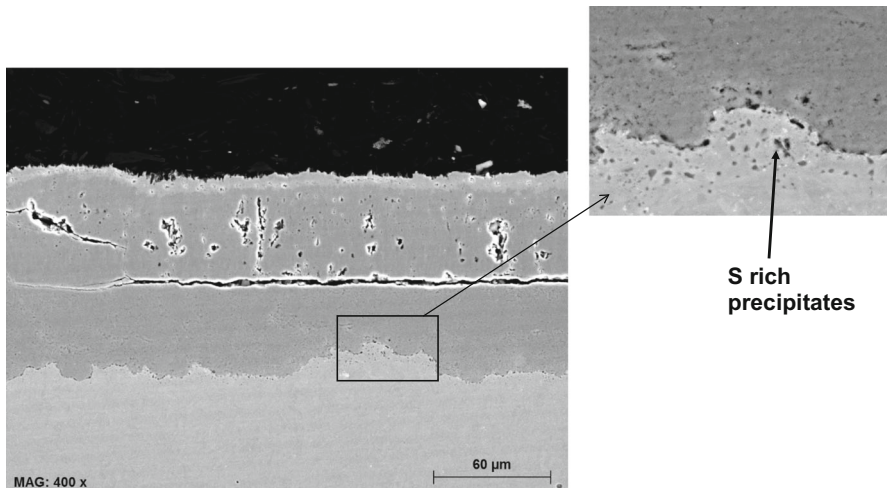


Fig. 17 P92 exposed to a model oxycombustion atmosphere (Table 1) at 650 °C for 168 h

mapping (Fig. 18a, b). Cr mapping also shows the present of a very rich Cr layer at the oxide-substrate interface on top of a Cr depleted substrate zone.

As under steam, both aluminide coatings are very protective for up to at least 1200 h at 650 °C under this atmosphere exhibiting very low weight gains as compared to uncoated P92. As observed under exposure to steam, the reference aluminide coating varies in microstructure due to diffusion and after 800 h widening of the cracks already present in the coating. Inside the cracks, S and O, Al and Fe could be detected by EDS point analysis but despite the fact that the crack reaches the substrate under the coating, no oxidation has taken place. This is certainly due to the presence of Al in this zone and the generation of a protective scale which will prevent substrate oxidation (Fig. 19). As observed during the steam oxidation test, the Cr enriched aluminide coating remained totally unaffected from both the microstructural and composition perspective (Fig. 20).

Test in Pilot Plant

Although for a relatively short duration (480 h) the reference aluminide coating was tested in CIUDEN's pilot fluidized bed boiler. Reheater P92 tube sections were coated and exposed to the oxycombustion atmosphere at 650 °C. Figure 21 shows the cross section of the coating covered by ash deposits including some Cl rich particle agglomerations. EDS analysis of the ashes indicated that they are mostly composed by oxides rich in Al (7–45 wt.%) with some Si and Fe. K (2–20 wt.%), Na (2–5 wt.%) and S (2–15 wt.%), the content varying depending on where the measurement was taken. The coating itself appear essentially unaffected, exhibiting only the phase transformations due to interdiffusing, as also observed in the laboratory experiments. Ashes deposited on these coatings do not appear to significantly react with the aluminide coating despite the presence of important

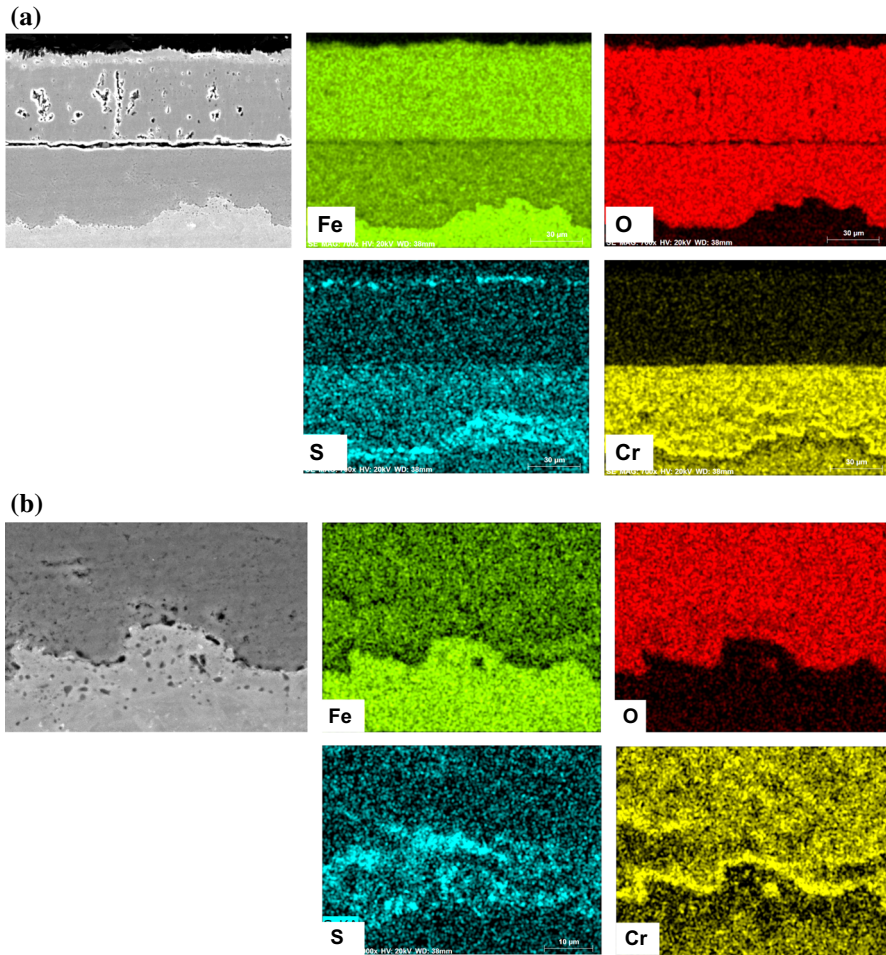


Fig. 18 EDS element mapping of the cross section of P92 exposed to oxycombustion atmosphere (Table 1) at 650 °C for 168 h. **a** Full oxide and **b** detail at the oxide-substrate interface

amounts of highly corrosive species such as S, Cl and alkali such as Na and K [19–22].

Discussion

The preliminary results indicate that both aluminide coatings (the reference and the Cr enriched version) protects from both steam and fireside corrosion. Longer exposures are of course required in order to be able to estimate their useful life but so far the results are promising. The advantages on these coatings is that they can

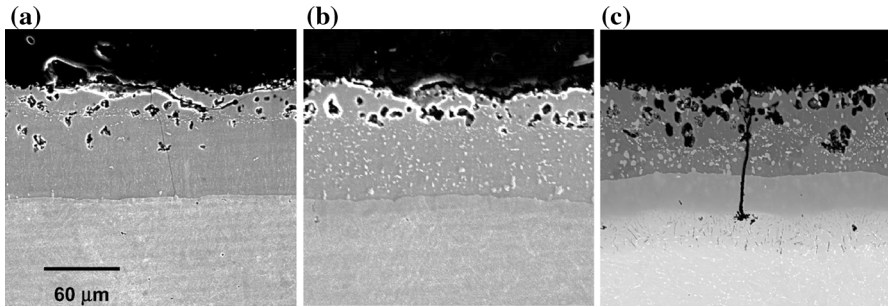


Fig. 19 Fe aluminide coating. **a** As deposited, **b** and **c** after 168 and 800 h of exposure to steam at 650 °C, respectively

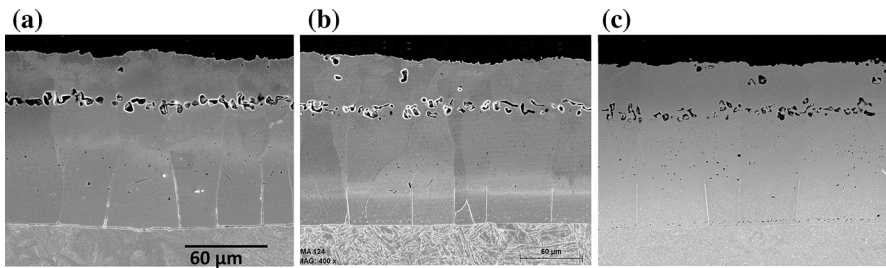


Fig. 20 Cr enriched aluminide coating. **a** As deposited, **b** and **c** after 168 and 800 h of exposure to steam at 650 °C respectively

perhaps be applied simultaneously on both inner and outer surfaces of boiler tubes or in the worst of the cases in two subsequent steps (inner and then outer surfaces).

The microstructure of the newly developed Cr enriched aluminide coating results from the higher temperature heat treatment, as faster Al–Fe interdiffusion takes place. No Fe_2Al_5 is present after 1 h at 1050 °C and cracks are therefore not developed during cooling. Moreover, a high degree of Kirkendall porosity develops at the coating substrate-interface, since Fe seems to diffuse outwards faster than Al inwards, as it happens with the reference aluminide coating but at much slower rates. In fact, the microstructure of the Cr enriched aluminide is very similar to that of the reference aluminide after long term exposure [11, 14]. AlN precipitates are present deep within the substrate into which Al has diffused, in the as heat treated coating, and are mostly larger than those observed in the reference aluminide coating heat treated at lower T, which only reach 4–5 μm within the substrate (Fig. 1). A heat treatment at temperatures higher than 740 °C will affect the mechanical properties of P92, but heat exchanger tubes can be reheat-treated to obtain the required ferritic-martensitic microstructure or alternatively, the coating process may be undertaken prior to the final tempering-annealing alloy treatment [10]. This coating seems very stable at 650 °C from the interdiffusion perspective, as after 2000 h at 650 °C no changes can be observed. The protective oxide appears stable to both steam and the model oxycombustion atmosphere. Testing at higher

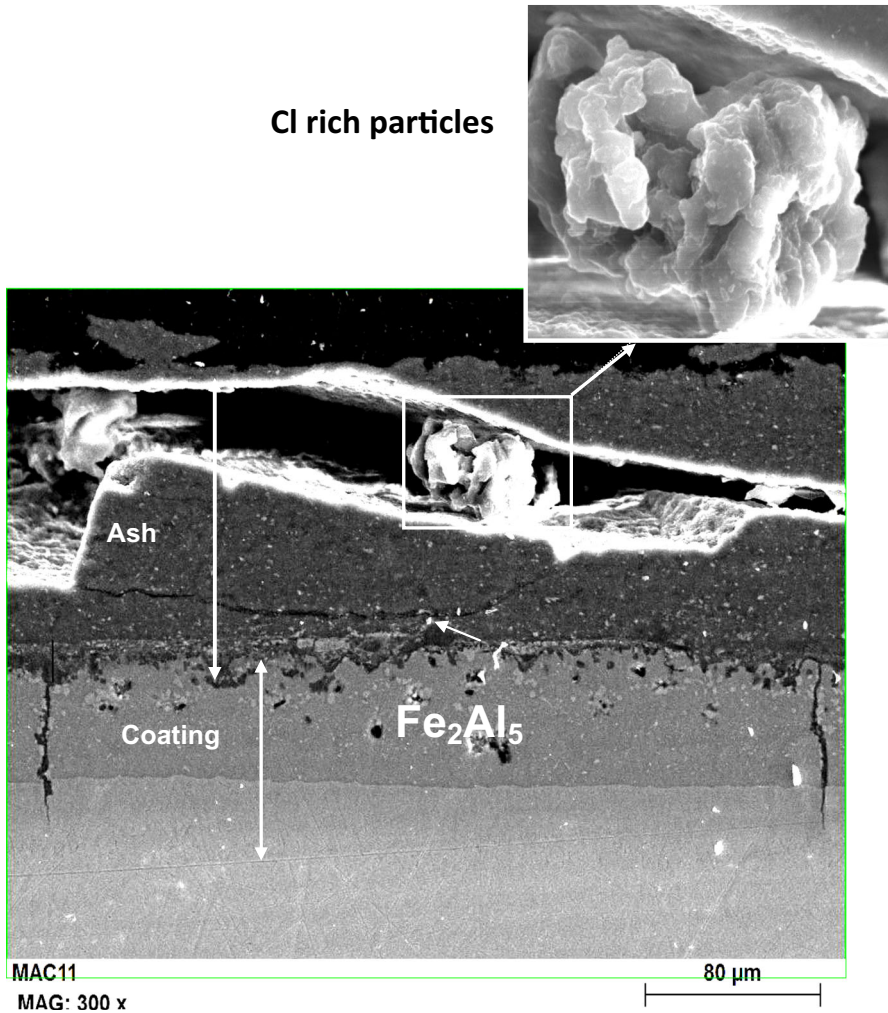


Fig. 21 Reference aluminide coating exposed for 20 days (480 h) to an oxycombustion from CIUDEN's pilot boiler at 650 °C

temperatures will be carried out in future, in order to accelerate Al depletion so that the Cr effect can be measured in a reasonable time, but on the basis of knowledge acquired by several researchers, the added Cr should reduce the critical amount of Al required to maintain a protective alumina scale [17].

The Ni aluminide coating deposited on P92 by aluminizing a previously diffused Ni layer forms a very interesting microstructure. P which was located at the most external surface of the Ni diffused coating, accumulates at the intermediate zone of the aluminide coating. This indicates that the coating has formed by outwards Ni diffusion like in low activity aluminides but in this case the process has occurred at 700 °C, a temperature typical of high activity aluminides [23]. Coating formation by

slurry application differs from traditional CVD and pack cementation aluminizing in that initially, aluminum melts and the diffusion process takes place by dissolving the substrate [13], in this case Ni into liquid Al until the corresponding intermetallics start solidifying. It would appear that P or P containing species, are not very soluble in molten Al since there is hardly any P on the top layer, and probably only as AlP as observed in the XRD pattern of this coating. The higher Al containing Ni_2Al_3 intermetallic has formed instead of NiAl because at the relatively low temperature interdiffusion rates are not high. The behavior of the top Ni_2Al_3 layer is very promising but internal oxidation must be eliminated. The obtained results seem to indicate that the presence of P at the coating substrate interface is detrimental either because it causes a weak interface between coating and substrate or because it accelerates oxidation rates. Instead of using Ni(P) electroless coatings, the next generations will be applied by Ni(B) or by electroplating pure Ni. Ni aluminides have been deposited on P92 first by electroplating Ni followed by pack aluminizing by Datta et al., and the results have been very promising for up to at least 3200 h under steam at 650 °C [24]. However, this coating developed an Fe_2Al_5 under the NiAl layer and cracks formed likely due to insufficient deposited Ni. If possible, electroless deposition is a simpler, lower cost coating process. However, if results are also disappointing, electroplated Ni will be employed.

Conclusion

Two new coatings have been developed for heat exchanger tubes. Both Cr and Ni aluminides can be applied in the internal as well as external surfaces of the tubes. The preliminary test results indicate that in particular, the Cr aluminide coating may represent an improvement over the pure aluminide coating as it does not exhibit cracks and degradation by diffusion is significantly slower. The Ni aluminide coating needed improvement in order to eliminate the possibility of internal oxidation likely related to the presence of P as a result of the Ni(P) electroless process. Longer exposure testing is ongoing. The reference aluminide coating was tested in a pilot oxycombustion boiler employing a mixture of biomass and coal as fuel for 480 h at 650 °C and no degradation was observed despite the presence of deposited ashes on the surface of the coating.

Acknowledgments The authors are grateful for the support by the Spanish Ministry of Economy and Competitiveness for financial support (ENE2011-29203-C02-01) as well as the EC (POEMA, G.A. No.: 310436). We also acknowledge ENDESA for supporting the pilot plant tests at CIUDEN and all members of the Metallic Materials Area at INTA for technical support.

References

1. T. U. Kern, in *9th Liège Conference on Materials for Advanced Power Engineering*, Vol. 29 (Liège, Belgium, 2010).
2. J. Hald, in *9th Liège Conference on Materials for Advanced Power Engineering*, Vol. 55 (Liège, Belgium, 2010).

3. CO₂ Capture Technologies, *Oxi Combustion with CO₂ Capture* (Global CCS Institute, Palo Alto, 2012). <http://www.globalccsinstitute.com/publications/co2-capture-technologies-oxy-combustion-co2-capture>.
4. T. Dudziak, T. Hussain, N. J. Simms, A. U. Syed and J. E. Oakey, *Corrosion Science* **79**, 184 (2014).
5. G. R. Holcomb, J. Tylczak, G. H. Meier, B. S. Lutz, K. Jung, N. Mu, N. M. Yanar, F. S. Pettit, J. Zhu, A. Wise, D. E. Laughlin and S. Sridhar, *Oxidation of Metals* **80**, 599 (2013).
6. G. Stein-Brzozowska, S. Babat, J. Maier, and G. Scheffknecht, in *Proceedings of Oxy-fuel Combustion Conference*, Vol. 2 (2011).
7. A. Hjörnhede, M. Montgomery, M. Bjurman, P. Henderson, and A. Gerhardt, in *9th Liege Conference for Advanced Power Engineering*, Vol. 1244 (Liège, Belgium, 2010).
8. B. Bordenet and F. Kluger, *Materials Science Forum* **595–598**, 261 (2008).
9. A. Agüero, V. González, M. Gutiérrez and R. Muelas, *Surface and Coating Technologies* **237**, 30 (2013).
10. A. Agüero, *Energy Materials* **3**, 35 (2008).
11. A. Agüero, V. González, M. Gutiérrez, R. Knödler, R. Muelas and S. Straub, *Materials and Corrosion* **62**, 561 (2011).
12. A. Agüero, M. Gutiérrez, R. Muelas, D. Plana, A. Román and M. Hernández, *Materials and Corrosion* **65**, 149 (2014).
13. A. Agüero, M. Gutiérrez and V. González, *Defect and Diffusion Forum* **289–292**, 243 (2009).
14. A. Agüero, K. Spiradek, M. Gutiérrez, R. Muelas and S. Höfner, *Materials Science Forum* **595–598**, 251 (2008).
15. Degradation and Protection of Materials under Oxyfuel atmospheres. Funded by MINECO (Spain), Project No. ENE2011-29203-C02-01 (2011–2013).
16. Production of Coatings for New Efficient and Clean Coal Power Plant Materials (POEMA), FP7 Program, G.A. No.: 310436, (2013–2016).
17. B. A. Pint, L. R. Walker and I. G. Wright, *Materials at High Temperatures* **21**, 175 (2004).
18. W. J. Quadakkers, P. J. Ennis, J. Zurek and M. Michalik, *Materials at High Temperatures* **22**, 47 (2005).
19. A. Zahs, M. Spiegel and H. J. Grabke, *Corrosion Science* **42**, 1093 (2000).
20. T. Hussain, A. U. Syed and N. J. Simms, *Oxidation of Metals* **80**, 529 (2013).
21. J. Pettersson, N. Folkesson, L.-G. Johansson and J.-E. Svensson, *Oxidation of Metals* **76**, 96 (2011).
22. S. Karlsson, J. Pettersson, L.-G. Johansson and J.-E. Svensson, *Oxidation of Metals* **78**, 83 (2012).
23. G. W. Goward and D. Boone, *Oxidation of Metals* **3**, 475 (1971).
24. Z. D. Xiang, D. Zeng, C. Y. Zhu, S. R. Rose and P. K. Datta, *Corrosion Science* **53**, 496 (2011).